Mechanistic Insights Into the Heterogeneity of Glucose Response Classes in Youths With Obesity: A Latent Class Trajectory Approach

Domenico Tricò,[1] Sarah McCollum,[2] Stephanie Samuels,[2] Nicola Santoro,[2,3] Alfonso Galderisi,[4] Leif Groop,[5] Sonia Caprio,[2] and Veronika Shabanova[2]

Diabetes Care 2022;45:1841–1851 | https://doi.org/10.2337/dc22-0110

OBJECTIVE

In a large, multiethnic cohort of youths with obesity, we analyzed pathophysiological and genetic mechanisms underlying variations in plasma glucose responses to a 180 min oral glucose tolerance test (OGTT).

RESEARCH DESIGN AND METHODS

Latent class trajectory analysis was used to identify various glucose response profiles to a nine-point OGTT in 2,378 participants in the Yale Pathogenesis of Youth-Onset T2D study, of whom 1,190 had available *TCF7L2* genotyping and 358 had multiple OGTTs over a 5 year follow-up. Insulin sensitivity, clearance, and β-cell function were estimated by glucose, insulin, and C-peptide modeling.

RESULTS

Four latent classes (1 to 4) were identified based on increasing areas under the curve for glucose. Participants in class 3 and 4 had the worst metabolic and genetic risk profiles, featuring impaired insulin sensitivity, clearance, and β-cell function. Model-predicted probability to be classified as class 1 and 4 increased across ages, while insulin sensitivity and clearance showed transient reductions and β-cell function progressively declined. Insulin sensitivity was the strongest determinant of class assignment at enrollment and of the longitudinal change from class 1 and 2 to higher classes. Transitions between classes 3 and 4 were explained only by changes in β-cell glucose sensitivity.

CONCLUSIONS

We identified four glucose response classes in youths with obesity with different genetic risk profiles and progressive impairment in insulin kinetics and action. Insulin sensitivity was the main determinant in the transition between lower and higher glucose classes across ages. In contrast, transitions between the two worst glucose classes were driven only by β-cell glucose sensitivity.

Central obesity is a strong modifier of diabetes risk, contributing to ever-increasing prevalence of youth-onset type 2 diabetes (T2D) in the U.S. (1,2). Despite the unprecedented rise in youth-onset T2D and prediabetes, very little is known about their pathophysiologies.

[1]*Department of Clinical and Experimental Medicine, University of Pisa, Pisa, Italy*
[2]*Department of Pediatrics, Yale University School of Medicine, New Haven, CT*
[3]*Department of Medicine and Health Sciences, "V. Tiberio" University of Molise, Campobasso, Italy*
[4]*Pediatric Endocrinology, Hôpital Necker-Enfants Malades, Paris, France*
[5]*Department of Clinical Sciences, Genomics, Diabetes and Endocrinology, Lund University, Malmö, Sweden*

Corresponding authors: Domenico Tricò, domenico.trico@unipi.it, and Veronika Shabanova, veronika.shabanova@yale.edu

Received 19 January 2022 and accepted 3 May 2022

This article contains supplementary material online at https://doi.org/10.2337/figshare.19859200.

Clinical trial reg. no. NCT01967849; clinicaltrials.gov

In adults, the risk of future T2D is strongly related to the shape of the plasma glucose curve during the oral glucose tolerance test (OGTT) (3–11). Similar observations were also described in adolescents with obesity who had normal glucose tolerance (NGT) or impaired glucose tolerance (IGT) (12–17). The authors of these studies reported that adolescents with a monophasic glucose curve during the OGTT have increased insulin resistance and decreased β-cell function compared with subjects with a biphasic glucose curve. Notably, adolescents with NGT are more likely to have a biphasic glucose curve with lower and earlier glucose peaks in contrast with the monophasic curve seen in adolescents with IGT. Previous research in adult and pediatric subjects that examined various glucose curve shapes was hampered by the use of predefined characteristics to designate the shape of the glucose curve; a short, 120 min OGTT without full absorption of the glucose load (18); and a mainly cross-sectional design.

In this study, we used the data-driven method of latent class mixed-effects modeling to identify subgroups of glucose response curves in youth, an approach that has been used to characterize glucose curves in the adult population over a more limited time frame of OGTT (8,10,11). We examined heterogeneity in glucose response curves during frequently sampled, 180-min OGTTs in a large U.S. multiethnic cohort of youths with obesity. A subgroup was followed longitudinally and had multiple OGTTs to assess the effects of age and changes in the main glucose homeostatic mechanisms on transition between classes. The objectives were to *1*) determine the prevalence of various glucose response classes in youths with obesity with NGT and IGT; *2*) identify potential differences in sex, race/ethnicity, and/or anthropometric factors among the various classes of glucose curves; *3*) determine the main pathogenic determinants of glucose responses among insulin sensitivity, insulin clearance, and the three main characteristics of β-cell function, including β-cell glucose sensitivity, rate sensitivity, and potentiation; and *4*) explore the association of the *TCF7L2* risk allele, the single strongest known genetic risk factor for youth-onset T2D (19–21), with the various glucose response classes.

RESEARCH DESIGN AND METHODS

Study Cohort

We analyzed cross-sectional OGTTs from 2,378 youths to derive latent classes of glucose trajectories among overweight/obese (BMI $\geq 85^{th}$ percentile for age and sex) children and adolescents without diabetes. This derivation sample came from our original multiethnic cohort of 2,585 obese youths participating in the Yale Pathogenesis of Youth-Onset T2D (PYOD) study (22). All participants underwent a 180 min, nine-point OGTT upon enrollment into the PYOD study. Among the derivation sample, 1,190 (50.0%) of 2,378 participants underwent *TCF7L2* genotyping and were included in the cross-sectional cohort. The rs7903146 single nucleotide polymorphism in *TCF7L2* was selected as a marker of genetic risk because no common variant that is widely shared across populations has a stronger effect in the pathogenesis of T2D (19). A subgroup of 358 (30.1%) of 1,190 participants elected to participate in the longitudinal study and had multiple OGTTs over a follow-up period of up to 5 years. The study cohort flow chart is shown in Supplementary Fig. 1.

A detailed medical and family history was obtained from all participants, and a physical examination was performed. Tanner stage was determined by a pediatric endocrinologist in 493 (41.4%) of 1,190 participants in the cross-sectional cohort and 230 (64.2%) of 358 in the longitudinal cohort (155 [67.4%] of whom had multiple assessments) who consented to the assessment of breast development in girls (23) and genitalia development in boys (24). The age distribution of the cross-sectional cohort by sex and Tanner stage is shown in Supplementary Fig. 2. To be eligible, participants needed to be ≤ 21 years of age and not taking any medications that affect glucose or lipid metabolism when enrolled.

The study was approved by the human investigations committee of the Yale School of Medicine. Parental informed consent and child assent were obtained from all participants before enrollment.

Latent Glucose Profile Classes in Youths With Obesity

Before the 180 min OGTT, all participants followed a weight maintenance diet, including at least 250 g of carbohydrates per day for 7 days, and were instructed to avoid strenuous physical activity. Following a 10–12-h overnight fast, participants arrived at the Yale Center for Clinical Investigation (20,21). Two baseline samples were obtained to measure plasma glucose, insulin, and C-peptide. Thereafter, a 1.75 g/kg of body weight dose of flavored dextrose (up to a maximum of 75 g) was given orally, and blood samples were obtained at 10, 20, and 30 min, then every 30 min up to 180 min to measure plasma glucose, insulin, and C-peptide levels. Glucose tolerance was defined according to American Diabetes Association criteria (25).

Insulin Sensitivity, β-Cell Secretory Function, and Insulin Clearance

Whole-body insulin sensitivity was assessed by OGTT-derived whole-body insulin sensitivity index (WBISI), which has been validated against the euglycemic-hyperinsulinemic clamp in adolescents with obesity (26). Insulin secretion rate (ISR) was estimated by C-peptide deconvolution (27). Parameters of β-cell function were calculated by mathematical modeling of ISR and glucose concentrations during the OGTT (28,29). Briefly, the relationship between glucose and ISR is the sum of two components. The first component represents the dependence of ISR on absolute glucose concentration. The quasilinear dose-response function relating the two variables is the β-cell glucose sensitivity slope. The static dose-response function is modulated by several factors (e.g. persistent hyperglycemia, gastrointestinal hormones), which are collectively modeled as a potentiation multiplying factor. The second insulin secretion component, β-cell rate sensitivity, represents the dynamic dependence of ISR on the rate of change of glucose concentration. Endogenous insulin clearance during the OGTT was calculated as the ratio between the areas under the curve (AUC) of ISR and plasma insulin (30–32).

Abdominal Fat Distribution

Abdominal MRI studies were performed using a Siemens Sonata 1.5-T system to quantify visceral and subcutaneous fat depots in 594 (49.9%) of 1,190 participants in the cross-sectional cohort (33,34). Hepatic fat fraction was measured using an advanced magnitude-based liver fat quantification MRI technique, the two-point Dixon, as modified by Fishbein and colleagues (35,36) and validated against liver biopsy in adolescents with obesity (37).

Genotyping

Genomic DNA was extracted from peripheral blood leukocytes. Genotyping for the single nucleotide polymorphism rs7903146 at *TCFL2* was performed with the use of matrix-assisted laser desorption ionization time-of-flight mass spectrometry on the MassARRAY platform (Sequenom) through the Yale Center for Genome Analysis (20).

Biochemical Analyses

Glucose was measured at bedside using the YSI 2700 Series STAT analyzer (Yellow Springs Instruments, Yellow Springs, OH). Plasma insulin was measured by radioimmunoassay (Linco, St. Charles, MO) that has $<$1% cross reactivity with C-peptide and proinsulin. Plasma C-peptide levels were determined by ELISA using ALPCO immunoassays (Salem, NH), with a 3.87% intraassay variability.

Statistical Analysis

Demographic and clinical characteristics of the derivation sample, cross-sectional cohort, and longitudinal cohort were summarized using counts with percentages, mean ± SD, or median (interquartile range [IQR]) and were compared using the χ^2 test for categorical variables and Student *t* test or Wilcoxon rank sum test for continuous variables.

Latent classes of glucose trajectories were modeled from the baseline OGTTs in the derivation sample using growth mixture modeling, with a random intercept for each child and an orthogonal polynomial (third degree) for the fixed effect of time (minutes of OGTT) (38,39). Growth mixture modeling was implemented using the package lcmm in R (38), and the posterior class probabilities were obtained using the package mixor in R (40). The number of latent classes was based on a model with the smallest Bayesian information criterion and Akaike information criterion, as well as the proportion of participants in each latent class with a posterior probability $>$0.70 (41). The 2 h glucose curve shape was also classified as monophasic, biphasic, or unclassified using the criteria proposed by Tschritter et al. (9) and replicated in youths (12).

Demographic and clinical characteristics and *TCF7L2* risk allele presence were compared among latent classes in the cross-sectional cohort using the χ^2 test and quantile regression with adjustment for age, sex, race/ethnicity, and BMI, as appropriate, and summarized using medians with 95% CIs. Model-based parameters of insulin sensitivity, β-cell secretion, and insulin clearance were summarized as median (IQR) and compared among the latent classes using the Kruskal-Wallis test followed by Dunn's multiple comparisons test. With standardized parameters of glucose homeostatic mechanisms as predictors, we modeled the log-odds of a higher latent class using ordinal logistic regression, and mean size of the glucose peak and predicted time to glucose peak during the OGTT using multivariable linear regression. Results were summarized as estimated slopes ($\hat{\beta}$ of standardized variables [std. $\hat{\beta}$]) ± SE, with partial R^2 values describing relative contributions of these predictors to class membership, glucose peak, and predicted time to glucose peak.

Using the longitudinal cohort, we estimated cumulative probabilities (risk) of latent class membership across age (square root of age in years), adjusting for sex and race/ethnicity, using generalized linear mixed-effects modeling with generalized log-odds (*glimmix* procedure, SAS 9.4; SAS Institute, Cary, NC). In a supportive analysis, we used available data on Tanner stage to model risk of latent class membership across the Tanner stages. In addition, we fitted a Markov multistate model for panel data (package msm in *R*) to obtain age-specific transition probabilities from one latent class to another, summarizing these using a Sankey diagram built with the package networkD3 in *R* (42). To investigate which parameters of glucose homeostasis drive observed changes in class membership over time (age in years), we first fitted $\log_e$(WBISI), $\log_e$(insulin clearance), square root(β-cell glucose sensitivity), and β-cell rate sensitivity using linear mixed-effects modeling in males and females separately, adjusting for race/ethnicity and BMI. Then, in separate generalized linear mixed-effects modeling regressions for each parameter of glucose homeostasis, we estimated and plotted odds ratios and 95% CIs of the longitudinal change in class membership for each SD increase in the parameter.

RESULTS

Characteristics of Derivation Sample, Cross-Sectional Cohort, and Longitudinal Cohort

Baseline characteristics of the derivation sample, cross-sectional cohort, and longitudinal cohort are shown in Supplementary Table 1. Compared with the derivation cohort, the cross-sectional cohort had more Hispanic participants and slightly lower BMI *z*-scores but was similar in age and sex composition.

The longitudinal cohort was slightly younger, had more girls and youths with IGT, but had similar weight and ethnic composition compared with the cross-sectional cohort. Among model-derived parameters, insulin sensitivity and clearance were statistically different between the cross-sectional and longitudinal cohorts.

Demographics and Clinical Characteristics by Latent Classes of Postload Glucose Profiles

Four latent classes of glucose response patterns were identified from the derivation sample. Classes were numbered from 1 to 4 on the basis of increasing AUCs for glucose. The number of participants included in each class decreased progressively from class 1 to 4, with class 1 having the greatest percentage of subjects (35%) and class 4 the lowest (11%) (Table 1). Age was the lowest in class 2, whereas the prevalence of girls and youth with Tanner stage 1 was the lowest in class 4. Although youth with advanced Tanner stages (4–5) were common in all latent glucose classes, youth with these two Tanner stages became highly represented in class 4, as did family history of T2D. Non-Hispanic White and African American participants were more represented in classes 3 and 4 and in classes 1 and 2, respectively, while the proportion of Hispanic participants was similar across classes. Notably, glucose tolerance status varied greatly by class, with class 1 having 99% NGT, class 2 having 82% NGT, class 3 having 75% NGT, and class 4 having only 7% NGT. Compared with class 1, participants in class 3 and 4 had the worst metabolic risk profiles, characterized by higher BMI, liver fat content, visceral and subcutaneous fat, HbA_{1c}, fasting and 2-h glucose, fasting insulin and C-peptide, triglyceride, and ALT levels.

Glucose, Insulin, and C-Peptide Patterns

The actual and predicted glucose pattern for each identified class is shown in Fig. 1*A*. There were only minor differences in fasting glucose concentrations across the four classes. Peak glucose concentration progressively increased from 7.3 mmol/L in class 1 to 10.1 mmol/L in class 4, while

Table 1—Clinical and metabolic characteristics of participants in the cross-sectional cohort (n = 1,190) stratified by latent glucose profile classes

	Class 1	Class 2	Class 3	Class 4
Participants	416 (34.96)	311 (26.13)	330 (27.73)	133 (11.18)
Age, years	13.27 (7.62, 18.60)	12.58 (7.51, 18.57)	13.56 (7.69, 18.78)	13.59 (8.68, 18.18)
Difference	Reference	−0.69 (−1.19, –0.21)	0.29 (−0.21, 0.93)	0.32 (−0.27, 0.85)
P	Reference	0.04	0.20	0.16
Sex				
Female	251 (60.34)	182 (58.52)	178 (53.94)	97 (72.93)
Male	165 (39.66)	129 (41.48)	152 (46.06)	36 (27.07)
Difference in female	Reference	−69 (−1.82)	−73 (−6.4)	−154 (12.6)
P	Reference	0.68	0.09	0.01
Tanner stage				
1	35 (8.41)	27 (8.68)	25 (7.58)	6 (4.51)
2–3	52 (12.5)	32 (10.29)	53 (16.06)	17 (12.78)
4–5	92 (22.12)	54 (17.36)	62 (18.79)	38 (28.57)
Missing*	237 (56.97)	198 (63.67)	190 (57.58)	72 (54.14)
Difference in 4–5	Reference	−38 (−4.75)	−30 (−3.33)	−54 (6.46)
P	Reference	0.67	0.25	0.17
Race/ethnicity				
Non-Hispanic White	142 (34.13)	99 (31.83)	142 (43.03)	58 (43.61)
African American	129 (31.01)	95 (30.55)	56 (16.97)	30 (22.56)
Hispanic/Latino	132 (31.73)	99 (31.83)	112 (33.94)	39 (29.32)
Other	13 (3.13)	18 (5.79)	20 (6.06)	6 (4.51)
P	Reference	0.35	0.00	0.13
Family history of T2D				
No	309 (74.28)	211 (67.85)	234 (70.91)	85 (63.91)
Yes	93 (22.36)	88 (28.3)	84 (25.45)	41 (30.83)
Difference in positive history	Reference	−5 (5.94)	−9 (3.1)	−52 (8.47)
P	Reference	0.07	0.35	0.05
BMI, kg/m^2	32.23 (25.59, 38.95)	32.37 (24.41, 40.42)	33.65 (25.83, 41.59)	33.38 (25.11, 41.82)
Difference	Reference	0.14 (−1.17, 1.47)	1.42 (0.24, 2.64)	1.15 (−0.48, 2.87)
P value	Reference	0.74	0.05	0.20
BMI *z*-score	2.28 (1.86, 2.68)	2.30 (1.78, 2.79)	2.37 (1.88, 2.84)	2.35 (1.83, 2.83)
Difference	Reference	0.02 (−0.08, 0.11)	0.09 (0.02, 0.16)	0.07 (−0.03, 0.16)
P	Reference	0.71	0.01	0.18
Weight class				
Overweight	43 (10.34)	32 (10.29)	24 (7.27)	12 (9.02)
Obese	373 (89.66)	279 (89.71)	306 (92.73)	121 (90.98)
P	Reference	0.99	0.19	0.78
Glucose tolerance status				
NGT	415 (99.76)	254 (81.67)	248 (75.15)	9 (6.77)
IGT	1 (0.24)	57 (18.33)	82 (24.85)	124 (93.23)
Difference in IGT	Reference	56 (18.09)	81 (24.61)	123 (92.99)
P	Reference	0.00	0.00	0.00
Glucose curve shape				
Biphasic	247 (59.38)	132 (42.44)	76 (23.03)	26 (19.55)
Monophasic	102 (24.52)	111 (35.69)	207 (62.73)	71 (53.38)
Unclassified	67 (16.11)	68 (21.86)	47 (14.24)	36 (27.07)
Difference between monophasic	Reference	9 (11.17)	105 (38.21)	−31 (28.86)
P	Reference	0.00	0.00	0.00
Hemoglobin A_{1c}[a], %	5.46 (5.1, 5.69)	5.56 (5.1, 5.84)	5.56 (5.15, 5.89)	5.66 (5.2, 5.99)
Difference	Reference	0.10 (0, 0.15)	0.10 (0.05, 0.2)	0.20 (0.1, 0.3)
P	Reference	0.00	0.01	0.00
Fasting glucose, mg/dL	88.3 (82.6, 94.6)	89.51 (82.7, 97.1)	91.9 (85.1, 99.6)	91.8 (84.5, 100.3)
Difference	Reference	1.2 (0.1, 2.5)	3.6 (2.5, 5.0)	3.6 (2.0, 5.6)
P	Reference	0.04	0.00	0.00
2-h glucose, mg/dL	101.8 (85.4, 119.0)	125.4 (106.2, 145.2)	125.2 (106.1, 145.5)	162.8 (141.4, 183.6)
Difference	Reference	23.6 (20.9, 26.2)	23.4 (20.7, 26.5)	61.0 (56.0, 64.6)
P	Reference	0.00	0.00	0.00

Continued on p. 1845

Table 1—Continued

	Class 1	Class 2	Class 3	Class 4
Glucose AUC, mg/dL × 180 min	102.9 (93.1, 113.8)	123.5 (111.5, 136.0)	127.1 (114.5, 140.3)	149.0 (136.8, 162.6)
Difference	Reference	20.5 (18.4, 22.2)	24.1 (21.4, 26.5)	46.1 (43.8, 48.7)
P	Reference	0.00	0.00	0.00
Fasting insulin,[a] μU/mL	25.44 (8.81, 41.28)	28.46 (9.76, 46.98)	32.44 (12.75, 51.28)	38.59 (16.51, 63.89)
Difference	Reference	3.02 (0.95, 5.70)	7.00 (3.95, 10)	13.16 (7.7, 22.61)
P	Reference	0.02	0.00	0.00
Fasting C-peptide,[a] pmol/L	996 (590, 1,391)	1,064 (590, 1,527)	1,188 (700, 1,665)	1,292 (746, 1,874)
Difference	Reference	68 (0.4, 136)	192 (110, 274)	296 (156, 483)
P	Reference	0.06	0.00	0.00
Total cholesterol,[b] mg/dL	152.6 (107.1, 197.3)	154.9 (103.8, 205.9)	155.1 (103.1, 206.8)	157.4 (102.9, 209.5)
Difference	Reference	2.3 (−3.3, 8.9)	2.5 (−3.9, 9.5)	4.8 (−4.2, 12.22)
P	Reference	0.45	0.48	0.13
HDL cholesterol,[b] mg/dL	43.47 (29.8, 58.04)	40.53 (25.22, 56.9)	41.09 (25.73, 57.3)	42.32 (25.42, 60.17)
Difference	Reference	−2.94 (−4.58, −1.15)	−2.38 (−4.07, −0.74)	−1.15 (−4.38, 2.12)
P	Reference	0.00	0.01	0.52
LDL cholesterol,[b] mg/dL	89.51 (47.91, 129.66)	90.81 (43.11, 136.86)	91.58 (44.35, 137.78)	90.03 (43.02, 135.75)
Difference	Reference	1.30 (−4.8, 7.2)	2.06 (−3.56, 8.11)	0.52 (−4.89, 6.08)
P	Reference	0.61	0.49	0.85
Triglycerides,[b] mg/dL	83.6 (20.4, 145.6)	95.7 (25.4, 164.9)	100.8 (28.5, 171.4)	98.9 (24.4, 177.4)
Difference	Reference	12.1 (5.0, 19.3)	17.2 (8.2, 25.8)	15.3 (4.0, 31.8)
P	Reference	0.00	0.00	0.12
ALT,[a] units/L	19.25 (10.49, 28.44)	20.25 (9.49, 31.44)	20.92 (10.49, 31.61)	23.25 (11.69, 34.7)
Difference	Reference	1.00 (−1, 3)	1.67 (−0.01, 3.17)	4.00 (1.19, 6.26)
P	Reference	0.11	0.06	0.00
SAT,[a] cm^2	440 (216, 650)	471 (197, 728)	473 (200, 729)	481 (202, 738)
Missing, *n***	206	167	170	66
Difference	Reference	32 (−20, 78)	33 (−16, 79)	41 (−14, 88)
P	Reference	0.11	0.05	0.02
VAT,[a] cm^2	53.5 (16.7, 92.3)	59.8 (17.1, 104.8)	63.2 (18.6, 110.0)	61.1 (16.1, 109.9)
Missing, *n***	206	167	169	66
Difference	Reference	6.3 (0.4, 12.5)	9.7 (2.0, 17.7)	7.6 (−0.6, 17.5)
P	Reference	0.05	0.01	0.12
Hepatic fat fraction	3.35 (0.00, 6.84)	3.76 (0.00, 7.93)	4.20 (0.00, 8.58)	4.83 (0.18, 9.85)
Median (IQR)	2.81 (1.98–4.79)	3.27 (2.19–5.46)	3.43 (2.59–6.02)	3.54 (3.13–6.67)
Missing, *n***	200	163	168	65
Difference	Reference	0.41 (0.00, 1.09)	0.85 (0.00, 1.74)	1.48 (0.18, 3.01)
P	Reference	0.16	0.03	0.04

Data are *n* (%) or median (95% CI) unless otherwise indicated. SAT, subcutaneous adipose tissue; VAT, visceral adipose tissue. [a]Adjusted for age, race/ethnicity, and sex. [b]Adjusted for age, race/ethnicity, sex, and BMI. *No differences were found between those with or without Tanner data in age at first visit, race/ethnicity, family history of T2D, obesity, IGT/NGT status, *TCF7L2* genotype, and latent glucose profile. More males (48%) than females (29%) had missing Tanner staging. **No differences were found between those with or without MRI data in family history of T2D, obesity, IGT/NGT status, *TCF7L2* genotype, and latent glucose profile class. Compared with participants with available MRI data, those with missing MRI data were younger (13.0 vs. 13.4 years) and more often female (62.8% vs. 56.0%) and non-Hispanic White (41.0% vs. 32.9%).

time to glucose peak was delayed in class 4 from 30 to 60 min. The glucose curves were maximally spread at 1 h. After this time point, the glucose curve of class 3 rapidly decreased, reaching the same glucose concentration of class 2 at 120 min and class 1 at 180 min. The corresponding insulin and C-peptide patterns are shown in Fig. 1*B* and *C*. Although insulin and C-peptide trajectories paralleled those of glucose levels in class 1, trajectories of C-peptide levels showed a much slower decrease in class 2 and 3. Notably, in class 4, both insulin and C-peptide peaked later than glucose (at 120 min).

Model-Based Parameters of Insulin Sensitivity, β-Cell Secretion, and Insulin Clearance

Insulin sensitivity progressively decreased from class 1 to 4 (Fig. 1*D*), while insulin secretion increased because of higher glucose levels (AUC 72 [IQR 58–90] nmol/m^2, 91 [73–116] nmol/m^2, 101 [79–123] nmol/m^2, and 114 [91–152] nmol/m^2, respectively; $P < 0.0001$) (Fig. 1*E*). Both measures of insulin secretion as a function of insulin sensitivity (Fig. 1*F*) and achieved plasma glucose levels (Fig. 1*G*) revealed a consistent decline in β-cell secretory function from class 1 to 4. β-Cell dysfunction

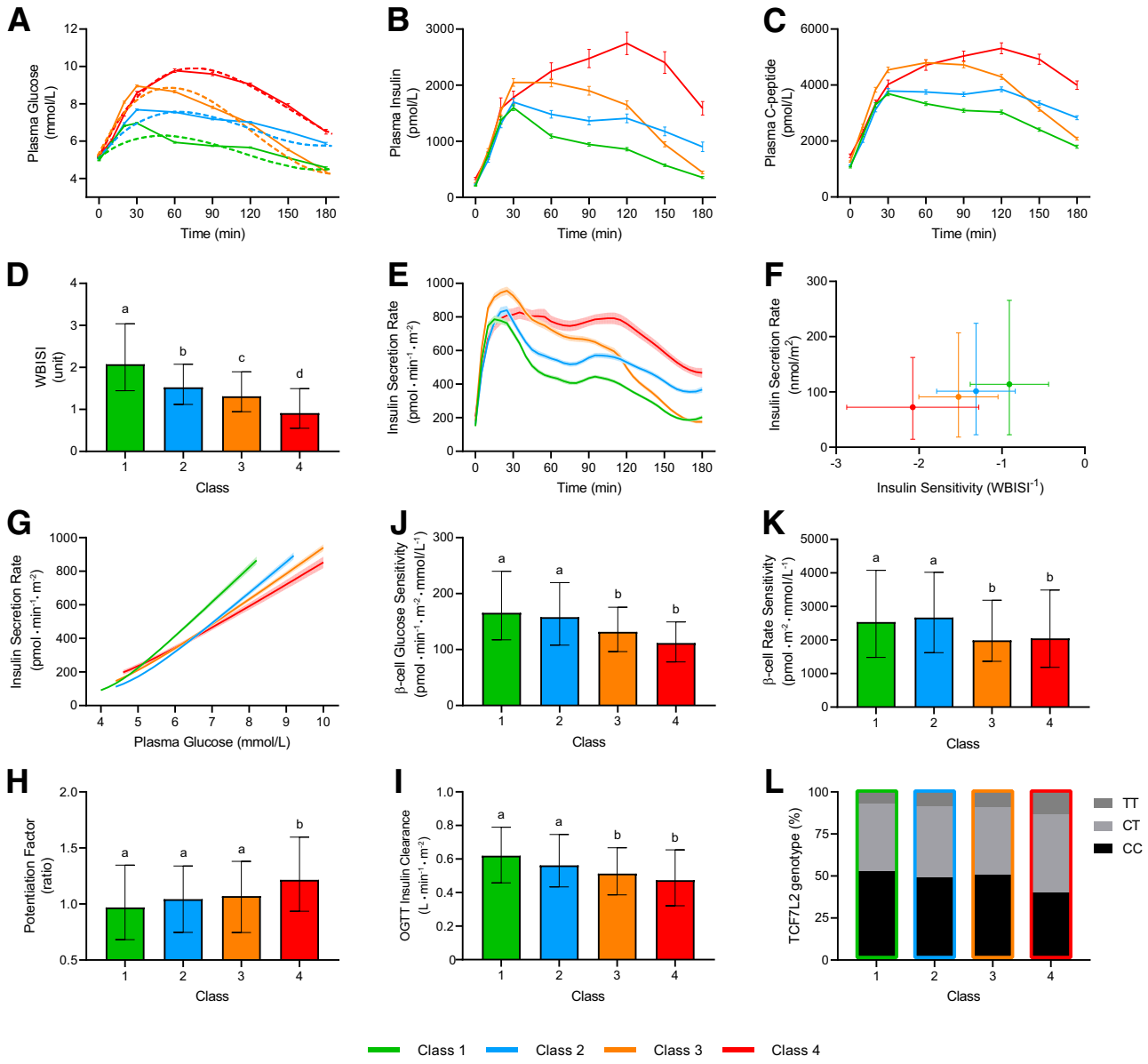

Figure 1—Observed (solid lines) and predicted (dashed lines) glucose profiles (*A*), plasma insulin (*B*), and C-peptide (*C*) profiles; WBISI (*D*), insulin secretion rate profile (*E*), total insulin secretion as a function of insulin sensitivity (*F*), and achieved plasma glucose levels (*G*); β-cell glucose sensitivity (*H*), rate sensitivity (*I*), and potentiation (*J*); total insulin clearance (*K*); and prevalence of the T risk allele for the common *TCF7L2* variant rs7903146 (*L*) in the four latent classes of glucose response patterns identified. Data are mean ± SEM (*A–C*, *E*, *G*) or median (IQR) (*D*, *F*, *H–L*). Different letters between groups indicate statistically significant differences ($P < 0.05$).

was due to deterioration in both β-cell glucose sensitivity (Fig. 1*J*) and rate sensitivity (Fig. 1*K*) and was partly compensated by increased potentiation (Fig. 1*H*) and reduced insulin clearance (Fig. 1*I*). The proportion of participants carrying the T risk allele for the common *TCF7L2* variant rs7903146 increased from class 1 to 4 (Fig. 1*L*), which is noteworthy because β-cell glucose sensitivity was lower in carriers of the CT/TT genotype (median 142 [95% CI 99–202] pmol · min^{-1} · m^{-2} · mmol/L^{-1}) compared with the CC genotype (152 [106–206] pmol · min^{-1} · m^{-2} mmol/L^{-1}; $P < 0.05$).

Relative Contribution of Main Pathophysiological Mechanisms to Class Membership

Among glucose homeostatic mechanisms, insulin sensitivity contributed the most (41.3% relative contribution) to individual class assignment (std. $\hat{\beta}$ ± SE 1.87 ± 0.13; $P < 0.0001$), followed by β-cell glucose sensitivity (28.4%; std. $\hat{\beta}$ 0.83 ± 0.07; $P < 0.0001$), insulin clearance (17.6%; std. $\hat{\beta}$ −0.89 ± 0.10; $P < 0.0001$), and β-cell rate sensitivity (12.8%; std. $\hat{\beta}$ 0.46 ± 0.07; $P < 0.0001$). The glucose peak size was determined 38.6% by insulin sensitivity (std. $\hat{\beta}$ −0.98 ± 0.05; $P < 0.0001$), 25.1% by β-cell glucose sensitivity (std. $\hat{\beta}$ −0.45 ± 0.03; $P < 0.0001$), 18.4% by insulin clearance (std. $\hat{\beta}$ 0.55 ± 0.05; $P < 0.0001$), and 17.9% by β-cell rate sensitivity (std. $\hat{\beta}$ −0.34 ± 0.03; $P < 0.0001$). Predicted time to glucose peak was determined 60.9% by insulin sensitivity (std. $\hat{\beta}$ −4.69 ± 0.34; $P < 0.0001$), 19.7% by insulin clearance (std. $\hat{\beta}$ 2.71 ± 0.34; $P < 0.0001$), and 19.0% by β-cell glucose sensitivity (std. $\hat{\beta}$ −1.47 ± 0.23; $P < 0.0001$), with only a minor (0.4%), nonsignificant relative contribution from β-cell rate sensitivity.

Longitudinal Analysis

In the longitudinal cohort, length of follow-up ranged from 6 to 60 months (median follow-up 29.3 [IQR 21.6–44.8] months), with 226 participants (63.13%) having two OGTTs, 93 (25.98%) having three OGTTs, and 39 (10.89%) having four or more OGTTs. Model-predicted probability to be classified as class 1 and 4 increased steadily with age, while probability to be classified as class 2 and 3 declined, after adjustment for sex and race/ethnicity (Fig. 2*A*). Similarly, model-predicted probability to be classified in the two extreme classes 1 and 4 increased across stages of pubertal development (Supplementary Fig. 3). Transition analysis among classes showed substantial variation across starting ages (Supplementary Fig. 4). Probability to be assigned to higher classes was consistently greater across ages in carriers of the rs7903146 CT/TT genotype than the CC genotype (class 1 vs. 3 $P = 0.06$; class 1 vs. 4 $P = 0.05$) (Fig. 2*B*). Insulin sensitivity ($P < 0.0001$) and insulin clearance ($P = 0.04$) showed a transient decline at ∼10–12 years of age, followed by a prompt recovery toward and above baseline values, with boys on average having higher values than girls (sex effect $P = 0.005$ and 0.001, respectively) (Fig. 3*A* and *B*). Conversely, the two main components of β-cell function, namely β-cell glucose sensitivity ($P = 0.04$) and rate sensitivity ($P = 0.03$), showed a linear decline in both sexes, with girls on average having higher glucose sensitivity than boys ($P = 0.03$) (Fig. 3*C* and *D*). When comparing standardized parameter estimates of glucose homeostatic mechanisms on age-related changes in class membership, a deterioration in insulin sensitivity was the strongest determinant in the transition from class 1 or 2 to higher classes, followed by changes in insulin clearance and β-cell glucose sensitivity (Fig. 3*E*). Rate sensitivity showed a smaller, but important effect in the transition from class 1 or 2 to class 3 or 4, but no effect in the transition between class 1 and 2. Transition between class 3 and 4 was explained only by changes in β-cell glucose sensitivity, while insulin sensitivity, insulin clearance, and rate sensitivity showed no significant effects.

CONCLUSIONS

In this study, we characterized the heterogeneity in glucose metabolism among a multiethnic cohort of children and adolescents with obesity for whom progression from prediabetes to diabetes may not be a foregone conclusion, and we identified which parameters of glucose homeostasis drive the risk of being in a specific latent glucose class over time. We used a data-driven approach rather than a predefined shape for glucose trajectories during the OGTT to discover the empirical trajectories of various latent glucose classes. The latent class trajectory approach also allowed us to investigate glucose changes over time while taking measurement error into account. Moreover, we provided a mechanistic explanation supporting the metabolic and genetic drivers underlying the newly described differences across classes using mathematical C-peptide modeling and *TCF7L2* genotyping.

Key findings include identification of four latent glucose profile classes, with classes 3 and 4 having the worst metabolic risk profiles characterized by a less favorable *TCF7L2* allele presence, greater adiposity and liver fat content, higher and delayed plasma glucose peaks during the OGTT, and progressive impairments in insulin sensitivity, β-cell function, and insulin clearance. Among the main glucose homeostatic mechanisms, insulin sensitivity contributed the most in determining class membership, glucose peak, and time to glucose peak, followed by β-cell glucose sensitivity. In longitudinal analysis, model-predicted probability to be classified in the two extreme classes (classes 1 and 4) increased with age, while the probability to be classified as class 2 or 3 decreased. The increase in extreme classes over time can be explained by two opposite phenomena described in our study that may identify

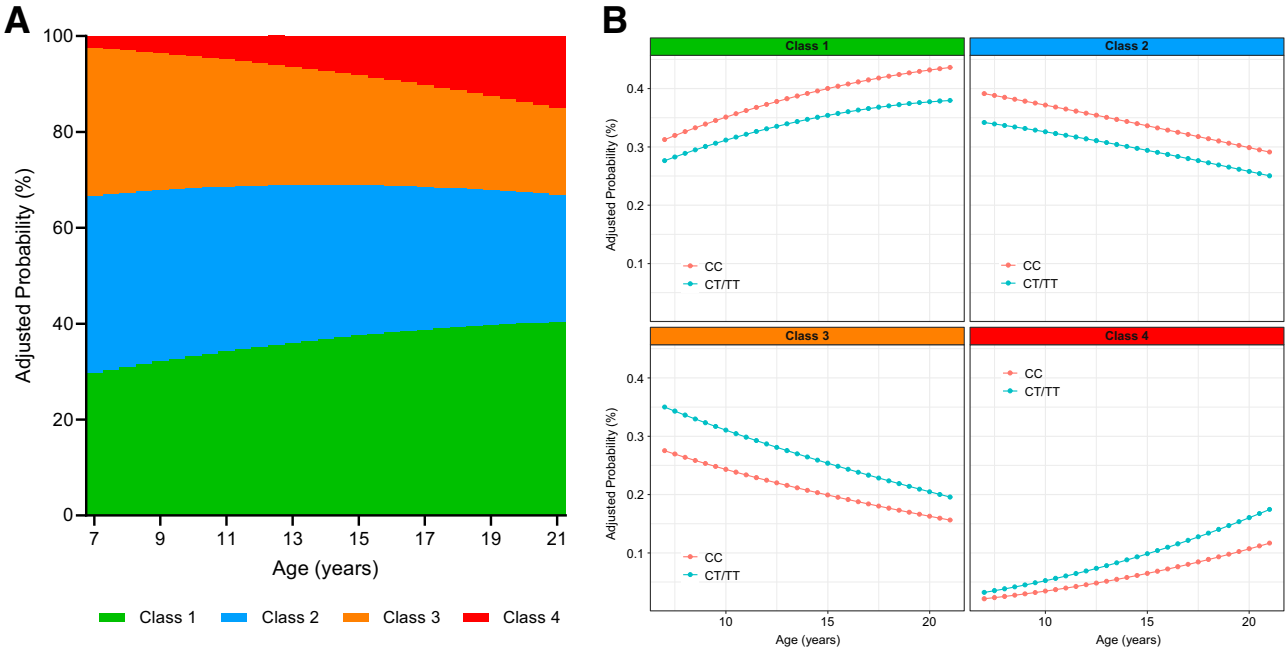

Figure 2—Model-predicted cumulative probability (risk) to be assigned to each of the four identified latent glucose pattern classes across ages in the longitudinal cohort (*A*) and in the subgroups of participants carrying the CT/TT or CC genotype (*B*). Probabilities are adjusted for sex and race/ethnicity.

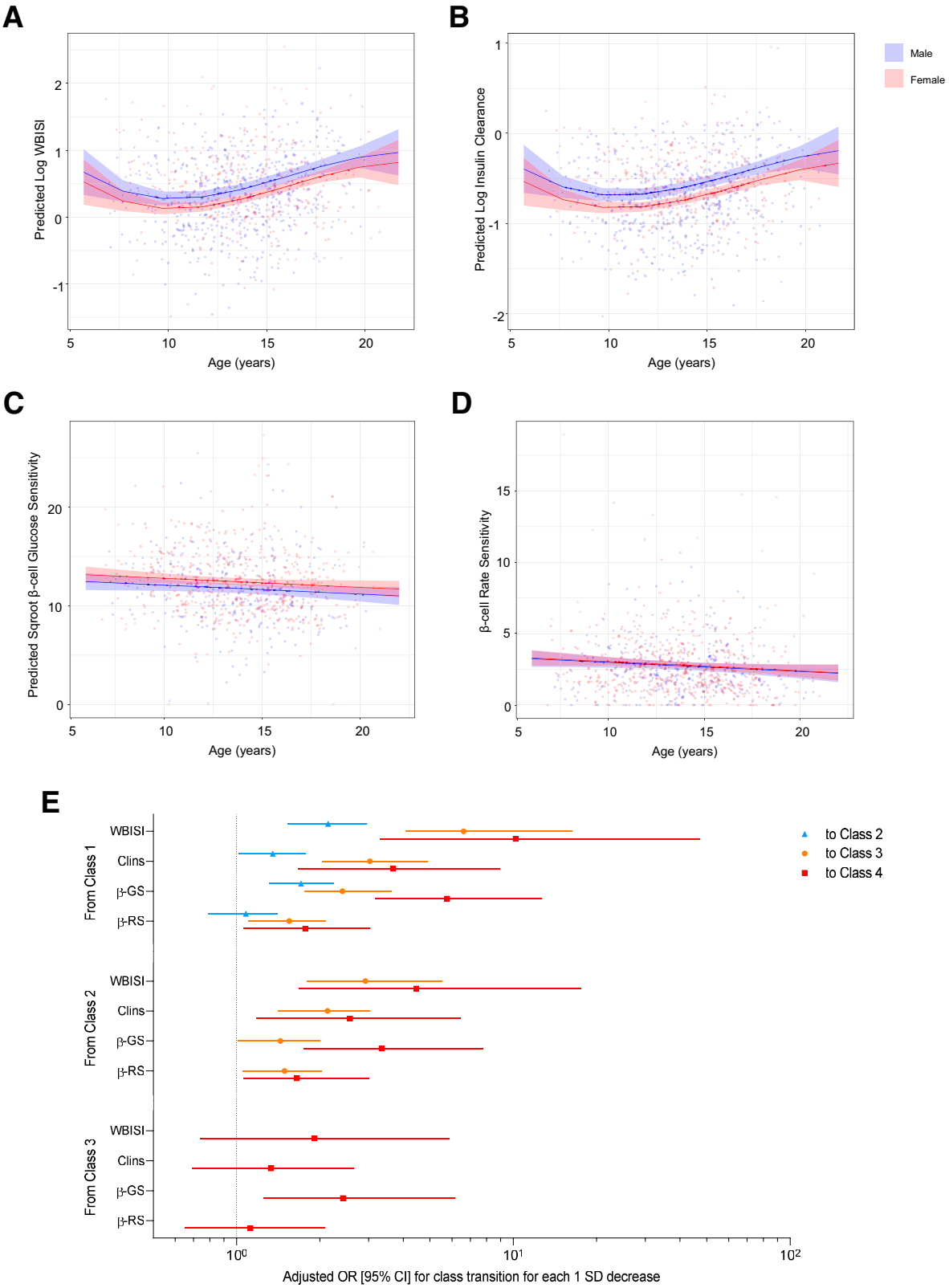

Figure 3—Longitudinal changes in insulin sensitivity (WBISI) (*A*), insulin clearance (Clins) (*B*), β-cell glucose sensitivity (β-GS) (*C*), and β-cell rate sensitivity (β-RS) (*D*) across ages in males and females, adjusted for race/ethnicity and BMI. Odds ratios (95% CIs) for the transition from lower to higher latent glucose pattern classes for each 1-SD decrease in WBISI, Clins, β-GS, and β-RS adjusted for sex and race/ethnicity (*E*). Sqroot, square root.

two different phenotypes of youths: *1*) recovery of insulin sensitivity and insulin clearance during adolescence, which enables the transition from class 2 to class 1, and *2*) progressive and irreversible decline in β-cell function, which is the main driver for transition from class 3 to 4. The worst phenotype, characterized by progressive β-cell dysfunction, may be

determined by the presence of the *TCF7L2* rs7903146 CT/TT genotype, which is associated with a much steeper increase across ages in the risk to be identified as glucose class 4 compared with the CC genotype (Fig. 2*B*). This finding is consistent with our previous reports in adolescents showing that each *TCF7L2* rs7903146 risk allele T is associated with β-cell dysfunction, reduced incretin effect, hepatic insulin resistance, and, eventually, increased odds for IGT/T2D, with an effect size greater than that reported in adults (20,21).

The pivotal role of β-cell function in transition across glucose response classes, independent from insulin resistance, has been recently confirmed in youth from the TrialNet Pathway to Prevention study (43). Specifically, the progression from a biphasic to a monophasic and, ultimately, to a continuous rise pattern of glucose response corresponding with decreasing β-cell function was reported to occur during progression to type 1 diabetes. However, this description does not allow for metabolic flexibility of youths with obesity at the individual level. We observed nonzero class membership transition probabilities for any given child. Importantly, although participants in class 4 featured all the essential metabolic defects for T2D development at enrollment (i.e., insulin resistance, β-cell dysfunction, reduced insulin clearance, genetic predisposition, increased intrahepatic fat), some changed class at follow-up to class 3, class 2, or even class 1 (Supplementary Fig. 4). This dynamic movement across glucose classes may be specific to youth, given that, in adults, a high stability of classes over time has been described (8). However, it should be noted that in the Restoring Insulin Secretion (RISE) study, neither adults nor adolescents showed different progression from IGT to diabetes or change in glycemic outcomes at 12 months by baseline glucose response curve (44). We speculate that transitioning among classes in our young population may explain the very high rate of reversibility of prediabetes and the difficulty in finding strong and stable risk markers for T2D in youth.

Wide age range (from 7 to 21 years), persistence of obesity and ectopic fat over time, and use of longitudinal 180 min OGTTs allowed us to shed new light on the long-standing question about the trajectories of changes in insulin resistance, insulin clearance, and β-cell function across the continuum of adolescence. We found that while insulin sensitivity decreases transiently, its rebound is not accompanied by improvements in β-cell function in youth with obesity. This uncoupling between the changes in insulin sensitivity and β-cell function, to the best of our knowledge, has not been previously reported in a large multiethnic cohort of children and adolescents with obesity.

Goran and Gower (45) showed a similar pattern of insulin sensitivity in a group of 60 children undergoing puberty, with insulin sensitivity decreasing at the onset of puberty and subsequently recovering at the end. Interestingly, β-cell function, expressed by disposition index, decreased linearly across Tanner stages in both non-Hispanic White and African American participants before and after adjusting for covariates (45). The Health Influences Puberty (HIP) study (46) compared longitudinal changes in insulin sensitivity and secretion during pubertal progression in youth with obesity and, notably, in a group of children with normal weight, reporting a significant impact of obesity on insulin sensitivity. In contrast with Goran and Gower's and our findings, Kelsey et al. (46) found that the disposition index was similar in the two groups, suggesting that youth with obesity were generally able to maintain adequate insulin secretion to compensate for insulin resistance. Despite their importance, these studies are limited by small sample sizes and should be replicated in larger groups of children.

Strengths and Limitations

A strength of our study is the active prospective surveillance of outcomes in a cohort of youths with variable features of obesity and metabolic impairment. Puberty appears to play a major role in the development of T2D in children (47), representing the ideal time frame for describing the natural history of youth-onset prediabetes. Thus, our study was performed in participants with a wide range of ages to include all stages of pubertal maturation. The longitudinal design, multiethnic composition of the cohort, wide range of body fatness represented, and objective measures of body composition and insulin/glucose dynamics are clear strengths of this study. Measurements of insulin sensitivity and secretion using standardized methods and mathematical C-peptide modeling were obtained together with genotyping for the most common genetic variant associated with β-cell dysfunction, providing global insights into the underlying physiological determinants of glucose classes. The longitudinal aspect of the study offers an understanding of dynamic changes and transitions across classes over time.

Despite these advantages, some limitations must be acknowledged. There was a relatively small number of participants <9 years of age, and we were unable to collect complete data regarding Tanner stage and abdominal fat composition. The lack of children with normal weights does not allow us to extend our findings to a healthy young population. In addition, the classification of glucose tolerance relied on only one OGTT per participant. OGTT may not establish glucose tolerance status reliably, given its limited reproducibility. However, we implemented several measures to mitigate this limitation in our study, including pretest dietary standardization, avoidance of strenuous physical activity, a child-friendly environment, and bedside analysis of glucose levels.

In conclusion, we identified four glucose response classes in youths with obesity characterized by progressive impairment in insulin sensitivity, secretion, and clearance. Insulin sensitivity was the main determinant of class assignment and transition between lower and higher classes across ages, followed by β-cell glucose sensitivity and insulin clearance. However, longitudinal transitions between the two worst glucose classes were only driven by changes in β-cell glucose sensitivity.

Acknowledgments. The authors thank Dr. Andrea Mari (National Research Council, Padova, Italy) for providing the tools for β-cell function modeling and for fruitful discussions. The authors also thank the patients and their families and acknowledge the Yale Center for Genome Analysis, Yale Center for Clinical Investigation, and Hospital Research Unit.

Funding. S.C. is funded by National Institutes of Health (NIH) grants R01-HD-40787, R01-HD-28016, R01-DK-111038, and K24-HD-01464. S.S. is supported by the National Institute of Diabetes and Digestive and Kidney Diseases (NIDDK) (NIH grant K12-DK-094714). N.S. is funded by NIH grants R01DK114504 and R01MD015974. This work was also made possible by National Center for Advancing Translational Sciences (a component of the NIH Roadmap for Medical Research) grant DK-045735 to the Yale Diabetes Endocrinology Research Center and by clinical and translational science award UL1-RR-024139.

The contents of this scientific contribution are solely the responsibility of the authors

and do not necessarily represent the official view of the NIH.

Duality of Interest. No potential conflicts of interest relevant to this article were reported.

Author Contributions. D.T. contributed to the study design, data analysis, interpretation of results, and drafting of the manuscript. S.M., and V.S. contributed to the study design, data analysis, interpretation of results, and drafting and editing of the manuscript. S.S., N.S., and A.G. contributed to the data collection, interpretation of results, and editing of the manuscript. L.G. contributed to the genotyping, interpretation of results, and editing of the manuscript. S.C. contributed to the funding, study design, data collection, interpretation of results, drafting and editing of the manuscript, and study supervision. D.T., and V.S. are the guarantors of this work and, as such, had full access to all the data in the study and take responsibility for the integrity of the data and the accuracy of the data analysis.

References

1. Lawrence JM, Divers J, Isom S, et al.; SEARCH for Diabetes in Youth Study Group. Trends in prevalence of type 1 and type 2 diabetes in children and adolescents in the US, 2001-2017. JAMA 2021;326:717–727
2. Viner R, White B, Christie D. Type 2 diabetes in adolescents: a severe phenotype posing major clinical challenges and public health burden. Lancet 2017;389:2252–2260
3. Abdul-Ghani MA, Williams K, DeFronzo R, Stern M. Risk of progression to type 2 diabetes based on relationship between postload plasma glucose and fasting plasma glucose. Diabetes Care 2006;29:1613–1618
4. Abdul-Ghani MA, Lyssenko V, Tuomi T, Defronzo RA, Groop L. The shape of plasma glucose concentration curve during OGTT predicts future risk of type 2 diabetes. Diabetes Metab Res Rev 2010;26:280–286
5. Manco M, Nolfe G, Pataky Z, et al. Shape of the OGTT glucose curve and risk of impaired glucose metabolism in the EGIR-RISC cohort. Metabolism 2017;70:42–50
6. Hulman A, Vistisen D, Glümer C, Bergman M, Witte DR, Færch K. Glucose patterns during an oral glucose tolerance test and associations with future diabetes, cardiovascular disease and all-cause mortality rate. Diabetologia 2018;61:101–107
7. Alyass A, Almgren P, Akerlund M, et al. Modelling of OGTT curve identifies 1 h plasma glucose level as a strong predictor of incident type 2 diabetes: results from two prospective cohorts. Diabetologia 2015;58:87–97
8. Hulman A, Witte DR, Vistisen D, et al. Pathophysiological characteristics underlying different glucose response curves: a latent class trajectory analysis from the prospective EGIR-RISC study. Diabetes Care 2018;41:1740–1748
9. Tschritter O, Fritsche A, Shirkavand F, Machicao F, Häring H, Stumvoll M. Assessing the shape of the glucose curve during an oral glucose tolerance test. Diabetes Care 2003;26:1026–1033
10. Obura M, Beulens JWJ, Slieker R, et al.; IMI-DIRECT Consortium. Post-load glucose subgroups and associated metabolic traits in individuals with type 2 diabetes: an IMI-DIRECT study. PLoS One 2020;15:e0242360
11. Hulman A, Simmons RK, Vistisen D, et al. Heterogeneity in glucose response curves during an oral glucose tolerance test and associated cardiometabolic risk. Endocrine 2017;55:427–434
12. Kim JY, Michaliszyn SF, Nasr A, et al. The shape of the glucose response curve during an oral glucose tolerance test heralds biomarkers of type 2 diabetes risk in obese youth. Diabetes Care 2016;39:1431–1439
13. Olivieri F, Zusi C, Morandi A, et al. "IGT-like" status in normoglucose tolerant obese children and adolescents: the additive role of glucose profile morphology and 2-hours glucose concentration during the oral glucose tolerance test. Int J Obes 2019;43:1363–1369
14. La Grasta Sabolić L, Požgaj Šepec M, Cigrovski Berković M, Stipančić G. Time to the peak, shape of the curve and combination of these glucose response characteristics during oral glucose tolerance test as indicators of early beta-cell dysfunction in obese adolescents. J Clin Res Pediatr Endocrinol 2021;13:160–169
15. Nolfe G, Spreghini MR, Sforza RW, Morino G, Manco M. Beyond the morphology of the glucose curve following an oral glucose tolerance test in obese youth. Eur J Endocrinol 2012;166:107–114
16. Galderisi A, Tricò D, Dalla Man C, et al. Metabolic and genetic determinants of glucose shape after oral challenge in obese youths: a longitudinal study. J Clin Endocrinol Metab 2020; 105:dgz207
17. Tricò D, Galderisi A, Mari A, Santoro N, Caprio S. One-hour post-load plasma glucose predicts progression to prediabetes in a multiethnic cohort of obese youths. Diabetes Obes Metab 2019;21:1191–1198
18. Tricò D, Mengozzi A, Frascerra S, Scozzaro MT, Mari A, Natali A. Intestinal glucose absorption is a key determinant of 1-hour postload plasma glucose levels in nondiabetic subjects. J Clin Endocrinol Metab 2019;104:2131–2139
19. Florez JC, Udler MS, Hanson RL. Chapter 14: genetics of type 2 diabetes. In *Diabetes in America*. 3rd ed. Cowie CC, Casagrande SS, Menke A, et al., Eds. Bethesda, MD, National Institute for Diabetes and Digestive and Kidney Disorders, 2018, 14-1–14-25
20. Galderisi A, Tricò D, Pierpont B, et al. A reduced incretin effect mediated by the rs7903146 variant in the *TCF7L2* gene is an early marker of β-cell dysfunction in obese youth. Diabetes Care 2020;43:2553–2563
21. Cropano C, Santoro N, Groop L, et al. The rs7903146 variant in the *TCF7L2* gene increases the risk of prediabetes/type 2 diabetes in obese adolescents by impairing β-cell function and hepatic insulin sensitivity. Diabetes Care 2017;40: 1082–1089
22. Galderisi A, Polidori D, Weiss R, et al. Lower insulin clearance parallels a reduced insulin sensitivity in obese youths and is associated with a decline in β-cell function over time. Diabetes 2019;68:2074–2084
23. Marshall WA, Tanner JM. Variations in pattern of pubertal changes in girls. Arch Dis Child 1969;44:291–303
24. Marshall WA, Tanner JM. Variations in the pattern of pubertal changes in boys. Arch Dis Child 1970;45:13–23
25. American Diabetes Association. 15. Diabetes advocacy: *Standards of Medical Care in Diabetes–2018*. Diabetes Care 2018;41(Suppl. 1):S152–S153
26. Yeckel CW, Weiss R, Dziura J, et al. Validation of insulin sensitivity indices from oral glucose tolerance test parameters in obese children and adolescents. J Clin Endocrinol Metab 2004;89:1096–1101
27. Van Cauter E, Mestrez F, Sturis J, Polonsky KS. Estimation of insulin secretion rates from C-peptide levels. Comparison of individual and standard kinetic parameters for C-peptide clearance. Diabetes 1992;41:368–377
28. Mari A, Ferrannini E. Beta-cell function assessment from modelling of oral tests: an effective approach. Diabetes Obes Metab 2008; 10(Suppl. 4):77–87
29. Tricò D, Mengozzi A, Nesti L, et al.; EGIR-RISC Study Group. Circulating palmitoleic acid is an independent determinant of insulin sensitivity, beta cell function and glucose tolerance in non-diabetic individuals: a longitudinal analysis. Diabetologia 2020;63:206–218
30. Mengozzi A, Tricò D, Nesti L, et al.; RISC Investigators. Disruption of fasting and post-load glucose homeostasis are largely independent and sustained by distinct and early major beta-cell function defects: a cross-sectional and longitudinal analysis of the Relationship between Insulin Sensitivity and Cardiovascular risk (RISC) study cohort. Metabolism 2020;105:154185
31. Tricò D, Galderisi A, Mari A, et al. Intrahepatic fat, irrespective of ethnicity, is associated with reduced endogenous insulin clearance and hepatic insulin resistance in obese youths: a cross-sectional and longitudinal study from the Yale Pediatric NAFLD cohort. Diabetes Obes Metab 2020;22:1628–1638
32. Tricò D, Galderisi A, Van Name MA, et al. A low n-6 to n-3 polyunsaturated fatty acid ratio diet improves hyperinsulinaemia by restoring insulin clearance in obese youth. Diabetes Obes Metab 17 March 2022 DOI:10.1111/dom.14695
33. Burgert TS, Taksali SE, Dziura J, et al. Alanine aminotransferase levels and fatty liver in childhood obesity: associations with insulin resistance, adiponectin, and visceral fat. J Clin Endocrinol Metab 2006;91:4287–4294
34. Umano GR, Shabanova V, Pierpont B, et al. A low visceral fat proportion, independent of total body fat mass, protects obese adolescent girls against fatty liver and glucose dysregulation: a longitudinal study. Int J Obes 2019;43:673–682
35. Fishbein MH, Gardner KG, Potter CJ, Schmalbrock P, Smith MA. Introduction of fast MR imaging in the assessment of hepatic steatosis. Magn Reson Imaging 1997;15:287–293
36. Leonetti S, Herzog RI, Caprio S, Santoro N, Tricò D. Glutamate-serine-glycine index: a novel potential biomarker in pediatric non-alcoholic fatty liver disease. Children (Basel) 2020;7:E270
37. Tricò D, Caprio S, Rosaria Umano G, et al. Metabolic features of nonalcoholic fatty liver (NAFL) in obese adolescents: findings from a multiethnic cohort. Hepatology 2018;68:1376–1390
38. Proust-Lima C, Philipps V, Liquet B. Estimation of extended mixed models using latent classes and latent processes: the R package lcmm. J Stat Softw 2017;78:1–56
39. Wardenaar KJ. Latent class growth analysis and growth mixture modeling using R: A tutorial for two R-packages and a comparison with Mplus. 28 January 2021 [preprint]. PsyArXiv: m58wx
40. Hedeker D, Gibbons RD. MIXOR: a computer program for mixed-effects ordinal regression analysis. Comput Methods Programs Biomed 1996;49: 157–176

41. Proust-Lima C, Séne M, Taylor JM, Jacqmin-Gadda H. Joint latent class models for longitudinal and time-to-event data: a review. Stat Methods Med Res 2014;23:74–90
42. Jackson CH. Multi-state models for panel data: ThemsmPackage for R. J Stat Softw 2011;38: 1–28
43. Ismail HM, Cleves MA, Xu P, et al.; Type 1 Diabetes TrialNet Study Group. The pathological evolution of glucose response curves during the progression to type 1 diabetes in the TrialNet pathway to prevention study. Diabetes Care 2020;43:2668–2674
44. Sam S, Edelstein SL, Arslanian SA, et al.; RISE Consortium; RISE Consortium Investigators. Baseline predictors of glycemic worsening in youth and adults with impaired glucose tolerance or recently diagnosed type 2 diabetes in the Restoring Insulin Secretion (RISE) study. Diabetes Care 2021;44:1938–1947
45. Goran MI, Gower BA. Longitudinal study on pubertal insulin resistance. Diabetes 2001;50: 2444–2450
46. Kelsey MM, Pyle L, Hilkin A, et al. The impact of obesity on insulin sensitivity and secretion during pubertal progression: a longitudinal study. J Clin Endocrinol Metab 2020;105:dgaa043
47. Arslanian SA. Type 2 diabetes mellitus in children: pathophysiology and risk factors. J Pediatr Endocrinol Metab 2000;13(Suppl. 6):1385–1394